VALENCIA
20 - 23 MAYO 2026
PALACIO DE CONGRESOS
38 CONGRESO NACIONAL
seram SEFERM

EXPLORING DE MANY FACES OF EXTRASKELETAL EWING SARCOMA

Mª Beatriz Sánchez de Lorenzo-Cáceres,MD; Carmen Nieves Hernández León, MD; Tania Marlem Chico González, MD; Juan Luis Conchuela Fumero, MD; Daniel Batista Martín,MD

Complejo Hospitalario Universitario de Canarias

BACKGRAOUND

- Ewing's sarcoma is a poorly differentiated tumor composed of small, round cells that primarily affects bones in children and young adults. Extraosseous Ewing's sarcoma (SEEE) is a similar tumor in morphology, but it affects extra-skeletal areas in older individuals, and accounts for approximately 20% of all Ewing’s sarcomas. With recent advances in molecular diagnostics, it is known that both derive from the same neuroectodermal cells and share the same translocations as bone Ewing's sarcoma.
- No differences have been described in histological, immunohistochemical, or molecular characteristics between bone Ewing's sarcoma and extraosseous forms. In all treatment guidelines, no differences in treatment are established between primary bone Ewing's sarcoma and extraosseous Ewing's sarcoma (EES); therefore, the treatment algorithm is similar.

PURPOSE OR LEARNING OBJECTIVE

- To describe CT, MRI, and PET-CT imaging features, locations, and outcomes of Extraskeletal Ewing Sarcoma (ESS).

PATIENTS AND METHODS

- Retrospective unicentric study from a tertiary Hospital of 12 EES patients from 2015-2022, evaluating demographic data, clinical presentation, location, size, contrast enhancement, 18-FDG avidity, and correlation with morphological, immunohistochemical, and molecular findings.

CASE 1:

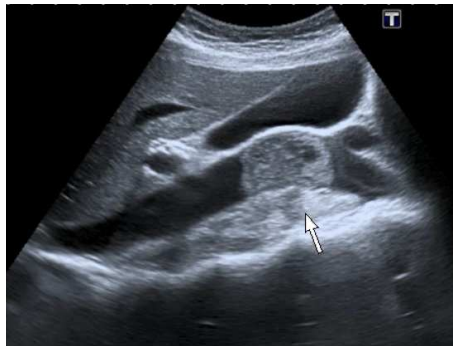

Figure 1: A 39-year-old woman with gross hematuria and flank pain lasting for 3 months. PMH: Congenital heart disease. Abdominal and pelvic ultrasound showing **thrombus** in the inferior vena cava, initial finding.

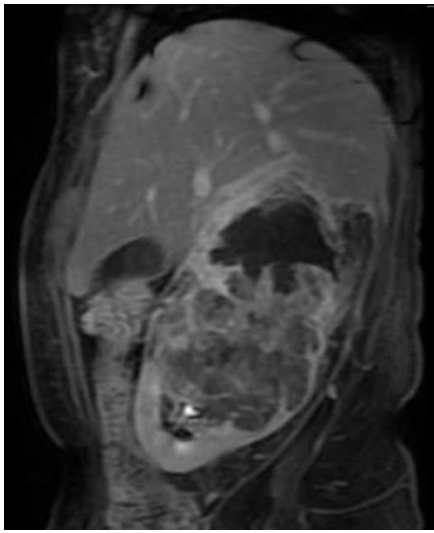

Figure 2: Sagittal T1-weighted MRI with intravenous contrast showed a large renal mass with evident tumor **necrosis**.

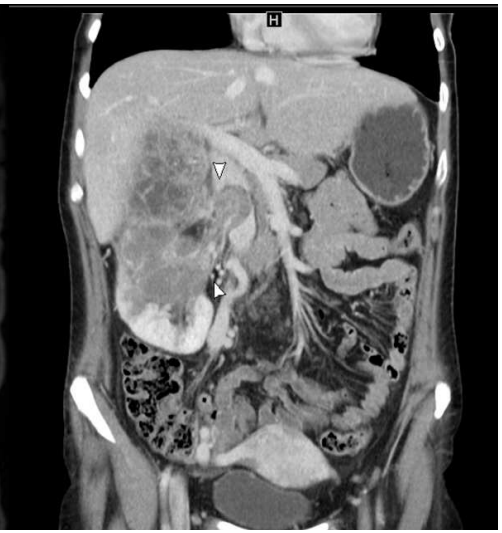

Figure 3: Coronal CT scan with IV contrast showing a large, heterogeneous, hypervascular mass with central **necrosis** in the upper third of the right kidney, measuring 15.4 x 11.2 x 10.7 cm with local invasion and **thrombosis** of the ipsilateral renal vein and the inferior vena cava with occlusive tumor thrombus. Multiple peritumoral and pelvic collateral vessels. Locoregional lymphadenopathy.

- Pathology report: **Extraosseous Renal Ewing Sarcoma** with **vascular invasion**. Immunohistochemical and molecular profile consistent with: **CD99+, FLI-1+, Ck+, sinaptofisina+.** EWS FISH study showed **no rearrangement.** Treatment: Patient was included in the Euro Ewing 2012 clinical trial, which evaluated chemotherapy and surgery, and was randomized to arm A with the VIDE regimen. Right nephrectomy with partial hepatic and diaphragmatic resection (due to local invasion) and endarterectomy of the inferior vena cava was performed. The postoperative specimen showed a poor response, with less than 50% tumor necrosis.

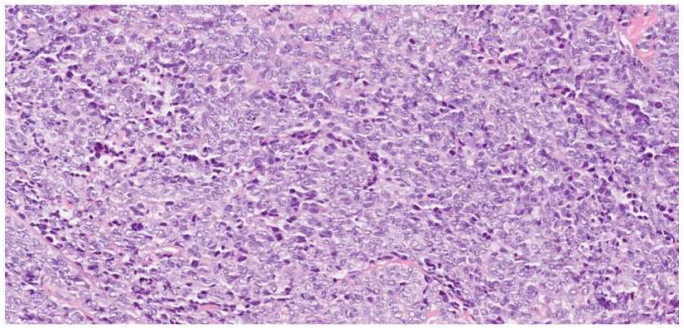

Figure 4: Pre-treatment biopsy sample, H&E stain (20x): A diffuse proliferation of small, round, blue, monomorphic cells is observed.

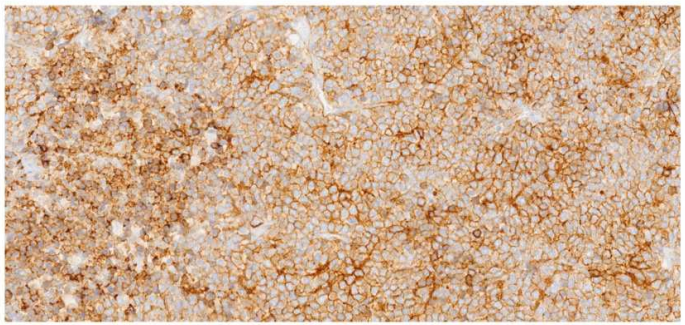

Figure 5: Typical membranous expression of CD99 observed in the tumor sample (20x).

Evolution: Following surgery, the patient presented with peritoneal, hepatic, and surgical bed progression, including invasion of the spinal canal and metastasis with a soft tissue mass in the clivus, leading to death. Palliative chemotherapy. Event-free-survival: 13 months.

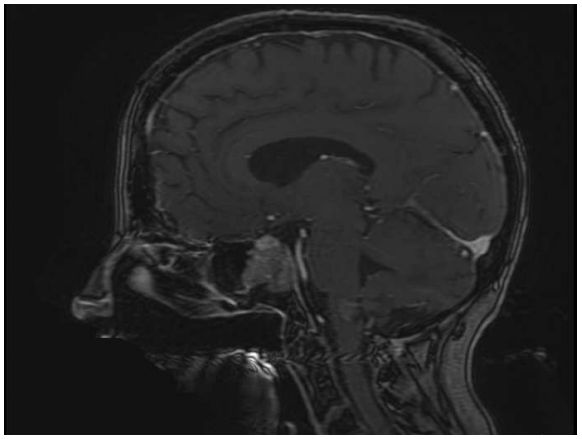

Figure 6: Contrast-enhanced brain MRI. Metastatic bone lesion in the clivus with an associated enhancing soft tissue mass measuring 2.8 x 2.3 cm, extending into the sphenoid sinus and the sella turcica–pituitary gland.

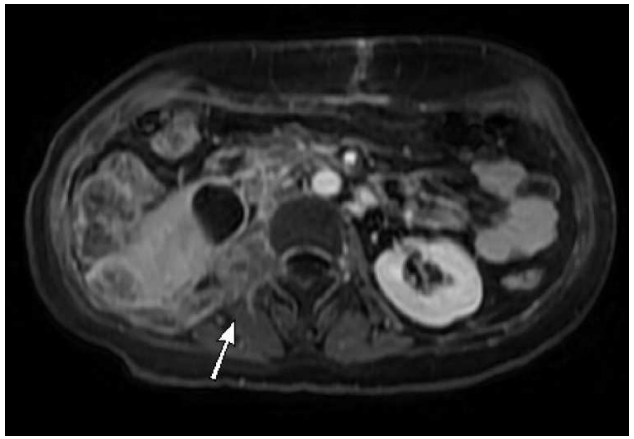

Figure 7: Contrast-enhanced renal MRI. Recurrence in the surgical bed with extension into the spinal canal.

CASE 2:

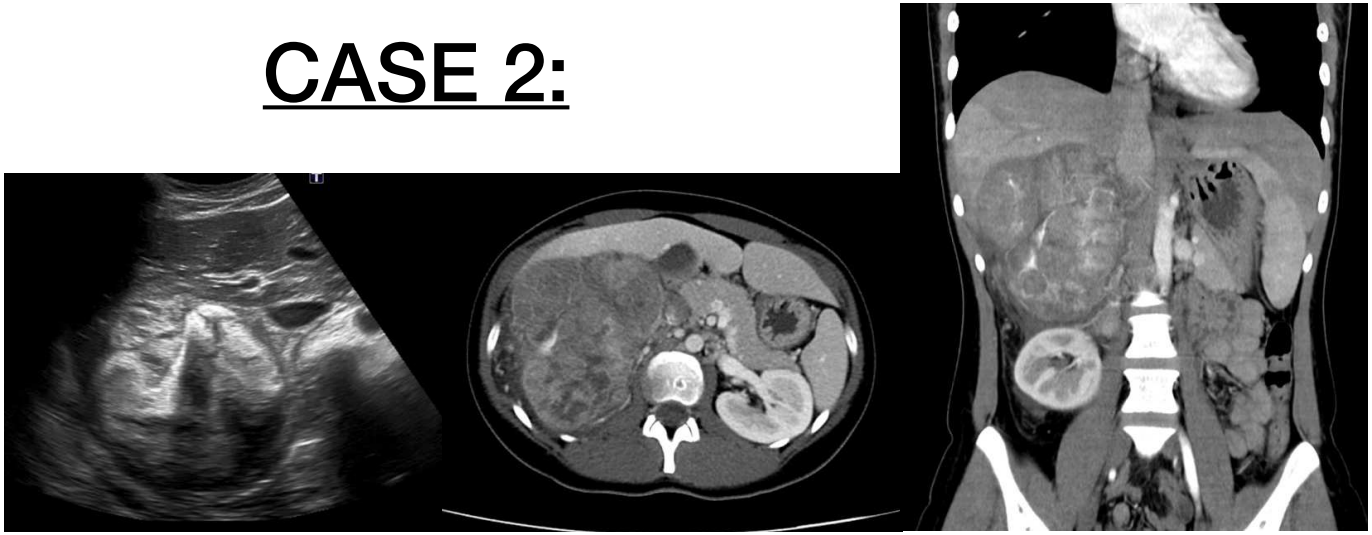

Figure 1: A 23-year-old woman presented to the emergency department with abdominal pain in the right hypochondrium/flank, fever, nausea, and vomiting. Weight loss and sweating. PMH: Childhood epilepsy. Urgent abdominal US revealed a **large heterogeneous mass** in the right adrenal region.

Figures 2 and 3: contrast-enhanced CT scan, confirming a hypervascular mass of 10,5 x 11,4 x 15,5 cm with areas of **tumoral necrosis.** This mass compresses and displaces the right kidney caudally, as well as the liver, pancreas, and the inferior vena cava, with which it is in close relation. Foci of calcifications. A small amount of free fluid is present. No secondary lesions were observed—differential diagnosis: Adrenocortical carcinoma, adult neuroblastoma, pheochromocytoma.

- Hormonal studies and urinary catecholamines were negative (ruling out functional pheochromocytoma).
- A right adrenalectomy was performed. Pathology report: Small round blue cells with marked necrosis, scant cytoplasm, and small monomorphic nuclei with fine chromatin. Foci of dystrophic calcification were present. Immunohistochemical and molecular profile consistent with: **Extraosseous Ewing Sarcoma:** membranous **CD99 positivity**, dot-like cytoplasmic CK positivity, **moderate nuclear FLI1**, and FISH showing **EWSR1 gene rearrangement.** Adrenal capsule not involved.
- A staging workup was performed, which revealed a normal LVEF. Additionally, bone scans, bone marrow aspirates, and biopsy results were negative. Localized disease without macroscopic residual after excisional biopsy. Not eligible for the EuroEwing trial. Treatment: Standard adjuvant treatment was administered with alternating VDCA/IE chemotherapy regimen and radiotherapy to the tumor bed. Fertility preservation was performed beforehand.
- Currently, the patient remains disease-free on follow-up annual evaluations. Event-free-survival: 70 months.

CASO 3:

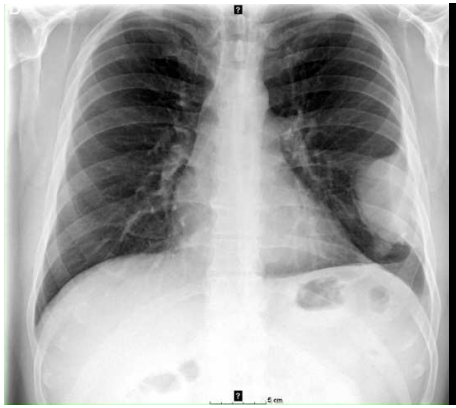

Figure 1: A 42-year-old man with increasing pain in the left hemithorax. X-ray showing a solid lesion in the left hemithorax of pleural origin, with ipsilateral atelectasis and pleural effusion.

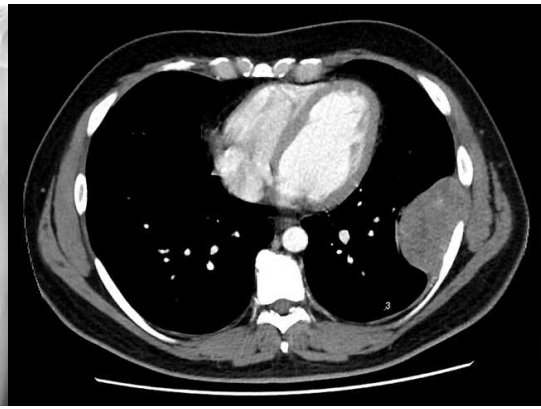

Figure 2: Contrast-enhanced CT scan of the posteroinferior left hemithorax showing a heterogeneous mass of 8 x 8,3 x 5 cm a broad pleural base, without evidence of chest wall invasion, the underlying ribs show no signs of lysis or erosion. Hypodense areas suggest **necrotic–cystic degeneratio**n.

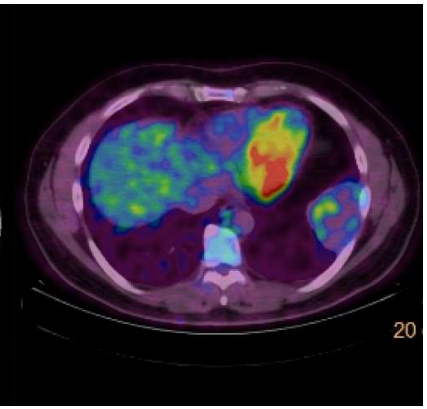

Figure 3: PET-CT showing a very heterogeneous pulmonary mass in the left lower lobe with moderate FDG uptake, invading the intercostal space.

Pathology report: confirmed **Extraosseous Ewing Sarcoma** of the chest wall. The immunohistochemical and molecular profile: strong and diffuse positivity for **CD99 and FLI-1. EWSR1–ERG rearrangement** was detected in NGS study. Treatment: Chemotherapy and surgery (left lower lobectomy and resection of the chest wall from the 6th to the 9th posterolateral ribs). The surgical specimen showed post-treatment changes consisting of <10% residual tumor, >90% tumor necrosis, and clear margins. Adjuvant chemotherapy and radiotherapy. The patient is currently in complete remission. Event-free-survival: 48 months.

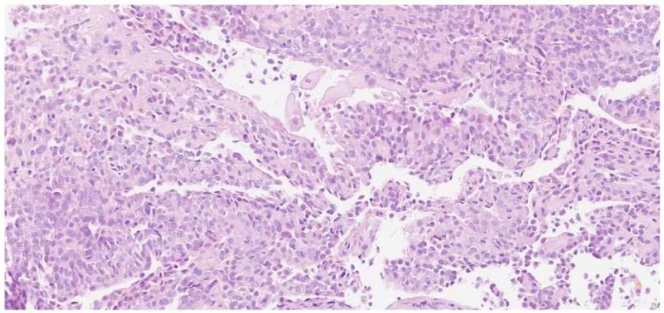

Figure 4: Diagnostic biopsy, H&E stain (20x): A proliferation of small, round, blue, monomorphic cells is observed.

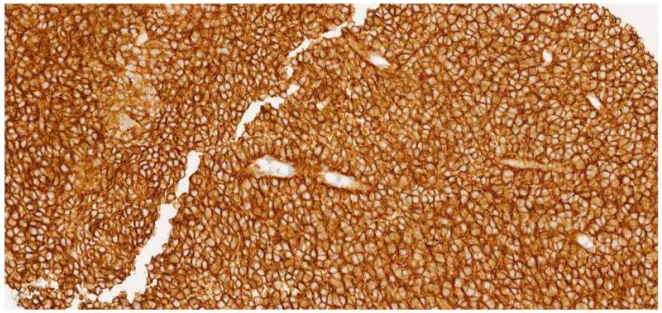

Figure 5: Typical membranous expression of CD99 observed in the tumor sample (20x).

CASO 4:

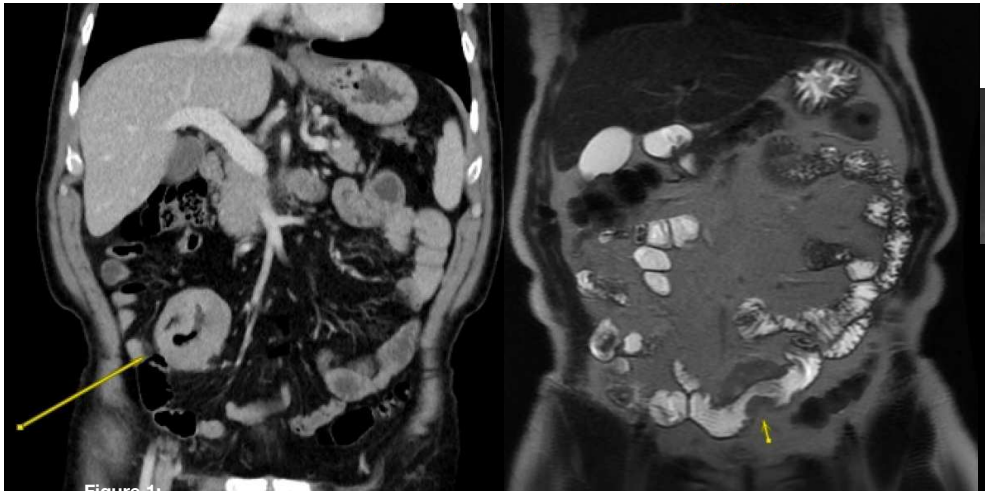

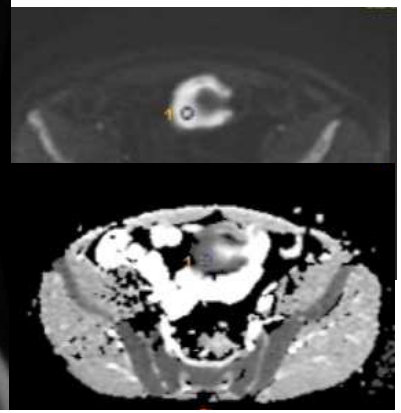

Figure 1: A 57-year-old man presented with diffuse abdominal pain lasting 6 months, associated with constipation, traces of blood, hyporexia, and weight loss. Contrast-enhanced CT of the abdomen and pelvis showing concentric mural thickening of a 6.2 cm segment of the terminal ileum, with mural thickening measuring 1.5 cm. Associated nodular densities in the mesenteric fat.

Figures 2 and 3: Coronal T2-weighted SSFSE BH MRI showing marked focal and concentric thickening of a distal ileal loop with significant diffusion restriction and pathological contrast enhancement (suspicious for lymphoma vs adenocarcinoma). No significant prestenotic dilatation is observed.

- Pathology report: revealed an **Undifferentiated Small Round Cell Sarcoma** involving all layers of the intestinal wall and mesenteric fat, with implants <4 mm (peritoneal carcinomatosis, T3N0M1). Immunohistochemistry suggested **Ewing Sarcoma: CK+, CK19+,CD99 membranous+,NSE+**; FISH and NGS confirmed **EWSR1 rearrangement.** Treatment: included surgery (segmental resection of the small intestine) and chemotherapy (VCD-IE regimen). Follow-up revealed peritoneal recurrence, ultimately resulting in death. Event-free-survival: 30 months.

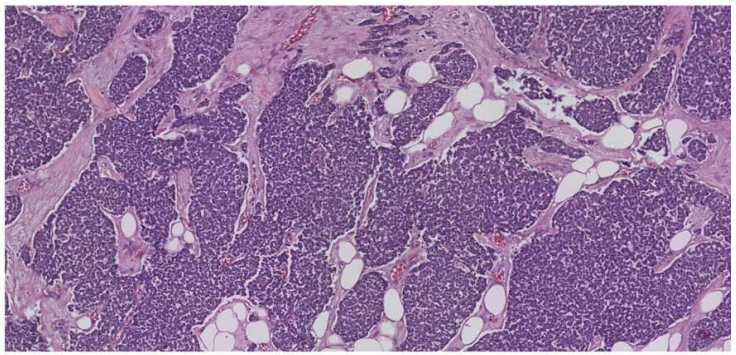

Figure 4: H&E stain (20x) of the surgical specimen showing a proliferation of small, round, blue, monomorphic cells infiltrating between the smooth muscle cells of the intestinal wall.

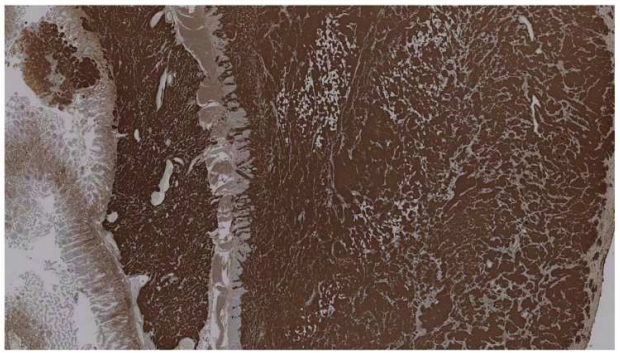

Figure 5: Typical membranous expression of CD99 observed in the tumor sample (20x).

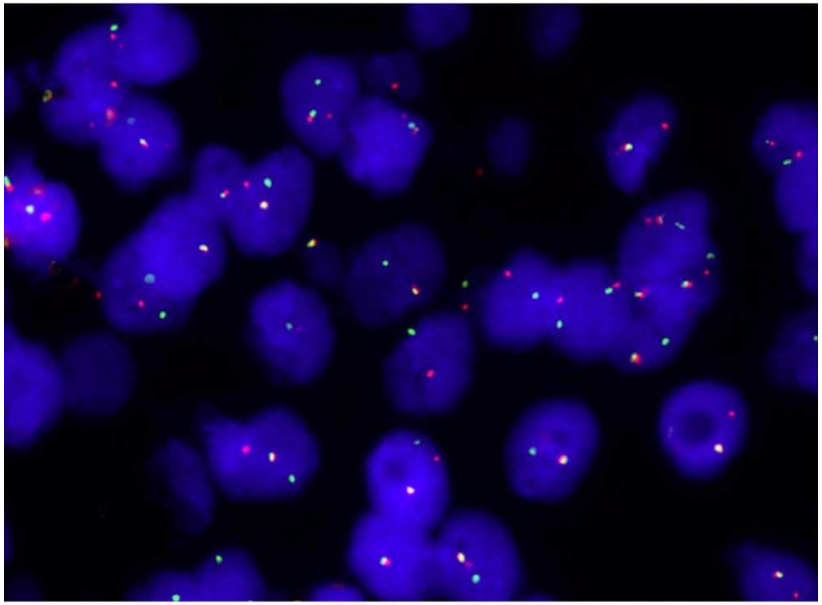

EWSR1 break-apart FISH analysis was performed, revealing rearrangement of the EWS gene (22q12).

Subsequently, Archer v2 NGS panel confirmed the presence of the EWSR1-FLI1 fusion

CASO 5:

A 39-year-old russian woman with left lumbar pain, hematuria, and urinary frequency. **Figure 1:** Sagittal contrast-enhanced MRI and **Figure 2**: axial T2 fat-suppressed images showing a large heterogeneous mass located at the upper pole of the left kidney measuring 7.6 x 7.7 x 10.5 cm encompassing vascular structures in the renal sinus with extension and invasion of the ipsilateral renal vein. No clear plane of separation with the adrenal gland, which is probably infiltrated. **Figure 3:** Contrast-enhanced CT scan with similar findings and pulmonary metastases. Stage T3N0M1.

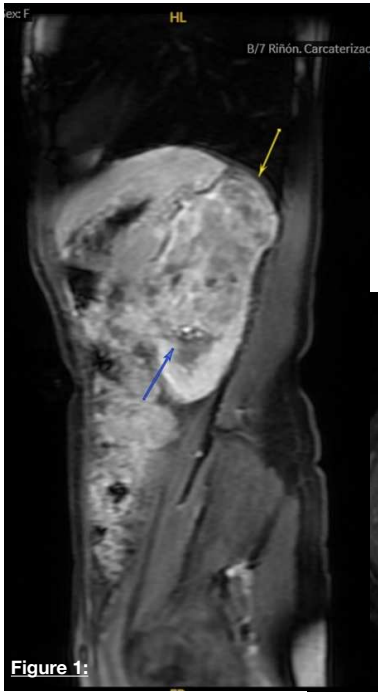

Figure 1:

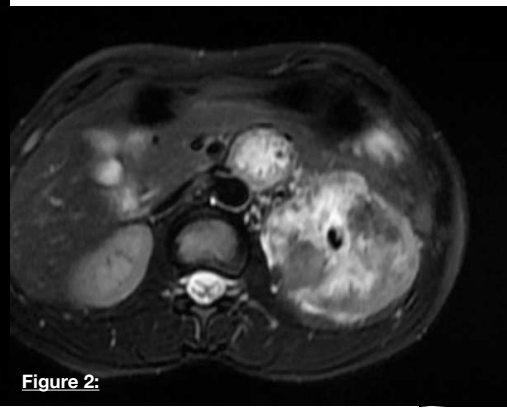
Figure 2:

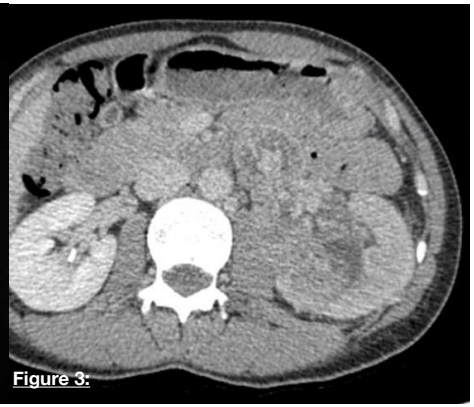
Figure 3:

- The pathology report showed Ewing Sarcoma with neoplastic infiltration of the renal sinus and tumor thromboembolism in the renal vein. Chronic lymphadenitis with vascular transformation of the lymph node sinuses (nodal angiomatosis) was also observed. Immunohistochemical and molecular profile: **CD99+, Fli1+,** CKAE1/AE3+. **EWS gene rearrangement** (22q12) was detected, with multiple hybridization signals of the rearranged allele.

- Treatment: Left radical nephrectomy was performed laparoscopically. The patient was a candidate for palliative chemotherapy with the VAC/IE regimen.

- Follow-up was not possible due to the patient being an immigrant. Outcome unknown.

CASO 6:

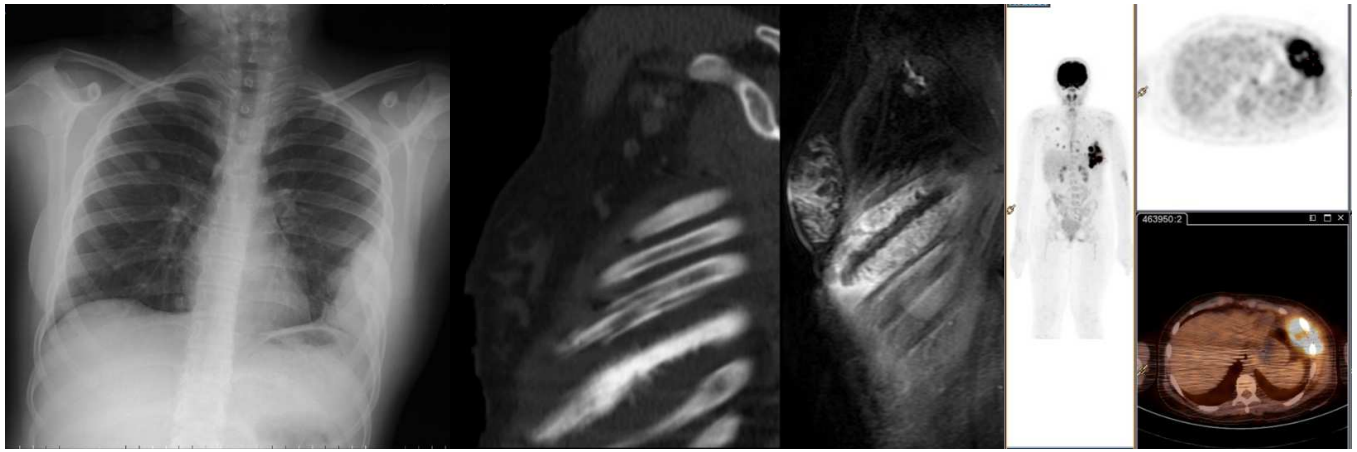

Figure 1: A 15-year-old girl with a history of hypoparathyroidism and hypercalcemia presented with 2 days of left costal pain, stiffness, and tremor of the left upper limb lasting minutes. Chest X-ray showing a solid costal lesion in the left hemithorax. Multiple pulmonary nodular lesions are consistent with metastases.

Figure 2: Contrast-enhanced CT and MRI of the chest showing a heterogeneous solid soft tissue mass measuring 8 x 4.7 cm with enhancement and areas of necrotic–cystic degeneration, centered on the left 6th rib, exhibiting signs of infiltration and marked destruction with lysis and spiculation.

Figure 3: PET-CT showing malignant tumor involvement of the left chest wall, multiple pulmonary metastases, and probable bone involvement in the left ischiopubic ramus. Mediastinal and axillary lymph nodes are suspicious for malignancy.

- Pathology report: round cell sarcoma with morphological, immunohistochemical, and molecular findings consistent with **Ewing Sarcoma: CD99+, Fli1+**. **FUS gene rearrangement** was detected by FISH. Treatment: Systemic treatment with chemotherapy was administered according to the SEHOP Ewing protocol and radiotherapy. The patient ultimately passed away. Event-free-survival: 15 months.

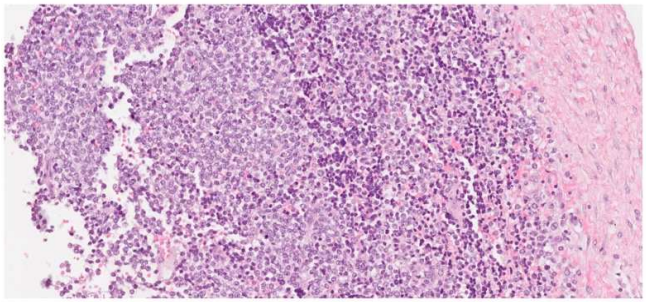

Figure 4: H&E stain (20x) showing a proliferation of small, round, blue, monomorphic cells

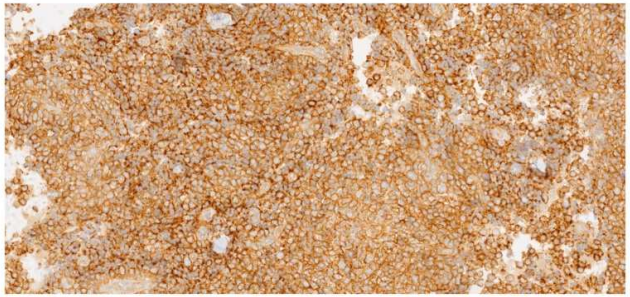

Figure 5: Typical membranous expression of CD99 observed in the tumor sample (20x).

CASO 7:

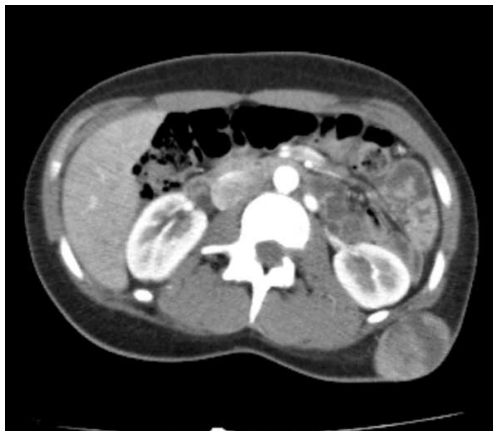

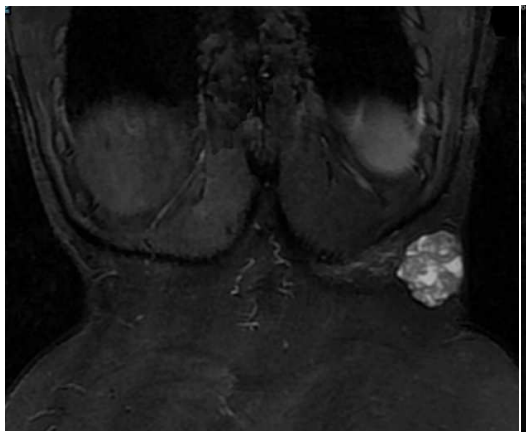

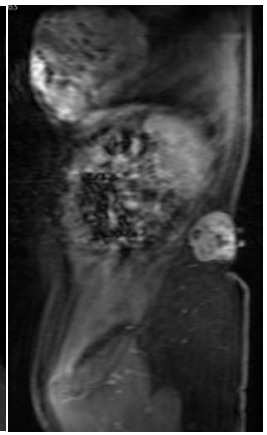

Figure 1: A 20-year-old woman with a visibly growing lesion on her back. Evaluated by dermatology and referred to plastic surgery for a lesion compatible with lipoma vs epidermoid cyst. Contrast-enhanced CT showing a heterogeneous mass. No evidence of distant disease.

Figure 2: Coronal STIR and **Figure 3:** Sagittal T1 contrast-enhanced MRI showing a soft tissue tumor located in the subcutaneous cellular tissue of the left paravertebral region, measuring 4.4 cm at its greatest diameter, with no signs of adjacent fascial infiltration (T1a). The lesion demonstrates heterogeneous contrast enhancement with areas of necrotic and cystic degeneration, suggestive of sarcoma.

- Pathology report: mesenchymal proliferation of small, round cells with morphological, immunohistochemical, and molecular findings: **CD99+ membranous, Ck+** consistent with localized **Extraskeletal Ewing Sarcoma. EWS gene rearrangement** (22q12) was detected. Treatment: The patient was enrolled in the EuroEwing trial, receiving 6 cycles of VIDE induction chemotherapy, followed by surgery, and then 8 cycles of VAI (GOOD RISK) or VAC (POOR RISK), with randomization to zoledronic acid +/- radiotherapy. She remains alive with no evidence of disease. Event-free-survival: 195 months.

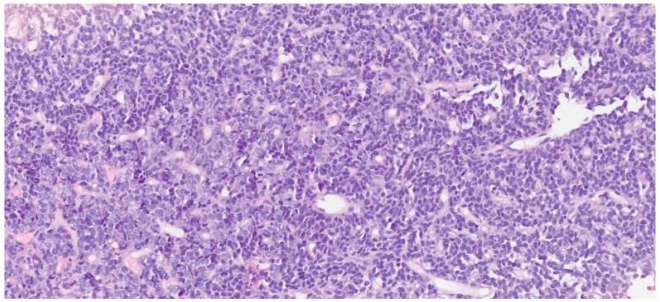

Figure 4: H&E stain (20x) showing a proliferation of small, round, blue, monomorphic cells.

Figure 5: Typical membranous expression of CD99 observed in the tumor sample (20x).

CASO 8:

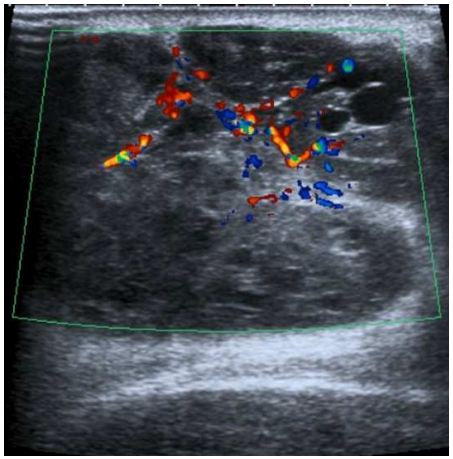

Figure 1: A 38-year-old woman with a growing shoulder lesion (previously excised infected sebaceous cyst, drained twice). US showing a highly vascularized heterogeneous mass with necrotic–cystic areas, located in the deep subcutaneous tissue in contact with the aponeurosis of the trapezius muscle.

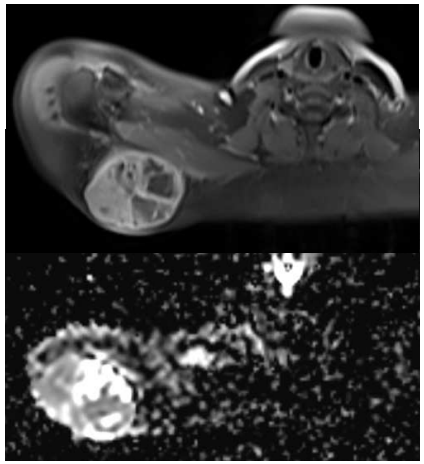

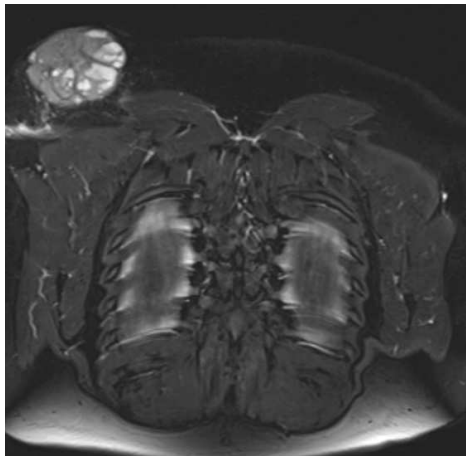

Figure 2: Axial T1 contrast-enhanced MRI, **Figure 3:** Axial DWI-ADC, and **Figure 4:** coronal STIR images showing a heterogeneous lesion with solid–cystic components in the subcutaneous tissue of the posterior aspect of the shoulder, measuring 7 x 5.5 x 4.7 cm. The solid component shows marked diffusion restriction. Areas of high T1 signal suggest hemorrhagic changes, and there is prominent enhancement with intravenous gadolinium. No metastases are observed on the remaining imaging studies.

- Pathology report: small round cell sarcoma with morphological, immunohistochemical, and molecular findings consistent with **Ewing Sarcoma. EWSR1 rearrangement** was detected. Treatment: The patient was treated with alternating VDC/IE chemotherapy, followed by surgery, and then continued with 5 additional cycles of VC/IE versus transplant, and subsequently local radiotherapy. She remains alive and disease-free. Event-free-survival: 71 months.

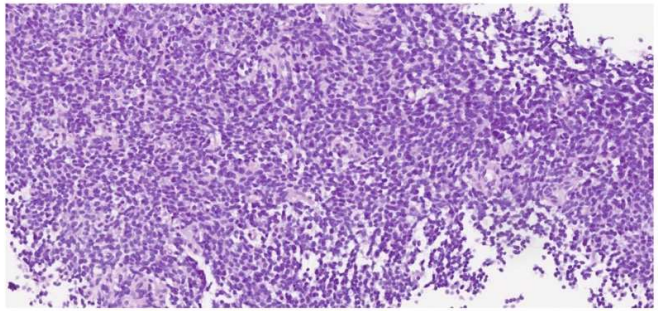

Figure 5: H&E stain (20x) showing a proliferation of small, round, blue, monomorphic cells.

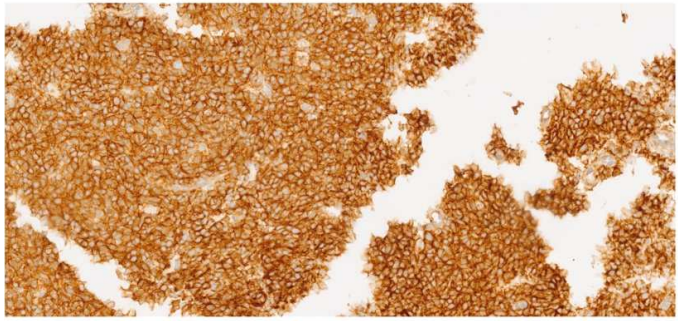

Figure 6: Typical membranous expression of CD99 observed in the tumor sample (20x).

CASO 9:

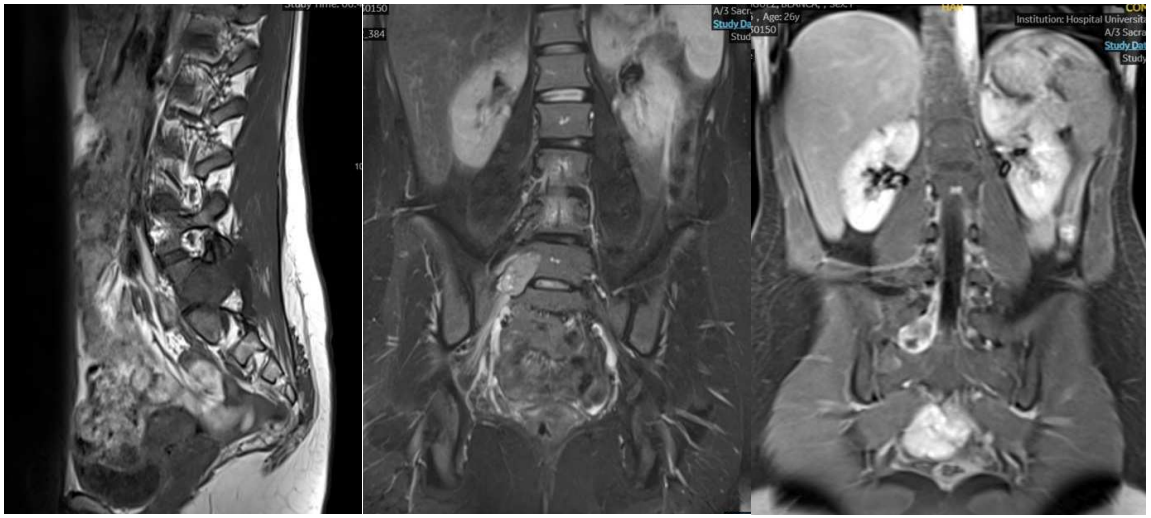

A 26-year-old woman with severe right buttock pain radiating to the right paravertebral and lumbar region, leg, calf, and sole. Progression to severe S1 radiculopathy with difficulty squatting and sensory alteration in the ankle and sole. **Figure 1:** Sagittal T1 MRI, **Figure 2:** coronal STIR, and **Figure 3**: coronal contrast-enhanced T1 MRI showing a lumbar tumor lesion occupying the right L5-S1 neural foramen with a solid component measuring 3 x 1.8 x 1.4 cm and a cystic-necrotic component. The lesion demonstrates heterogeneous contrast enhancement and diffusion restriction on DWI. It extends through the spinal canal, occupying the right lateral recess to the retroperitoneal-pelvic space. Bone remodeling is present without apparent infiltration. No distant lesions suggestive of metastases.

- Pathology report: proliferation of small, round cells consistent with lumbosacral **Ewing Sarcoma. FISH for EWS shows gene rearrangement.**

- Treatment: Surgery (L5-S1 laminectomy) was suboptimal due to field contamination and residual tumor persistence. The patient is a candidate for induction chemotherapy with alternating VDCA/IE for 9 cycles.

- A surgical biopsy was performed on the residual tumor, ± proton therapy was planned afterward. Pathology results were negative, possibly due to the tumor area being missed. Treatment: Given the risks and high morbidity, further surgery was not performed. The decision was made to continue intensified chemotherapy before proton therapy.

- The patient is currently under follow-up. Event-free-survival: 38 months.

CASO 10:

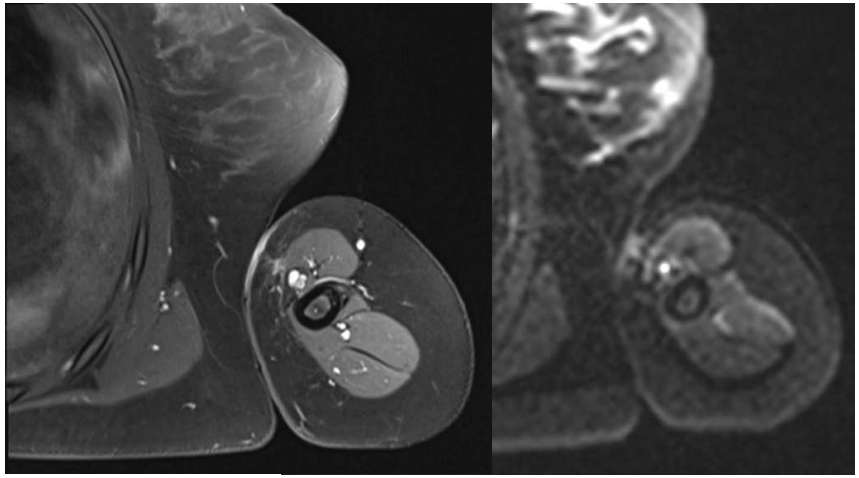

A 15-year-old girl with a nodule in the cutaneous plane of the inner left forearm. Ultrasound and MRI were performed at a private center (images not available), with suspicion of lipoma vs leiomyoma. Outpatient excision/biopsy surgery was performed, with pathological diagnosis of Extraskeletal Ewing Sarcoma (EES). Margins were positive. A lump is now palpable in the scar area. **Figure 1:** Axial T1 contrast-enhanced MRI and **Figure 2:** axial DWI showing nodular enhancement in the caudal aspect of the scar with areas of diffusion restriction.

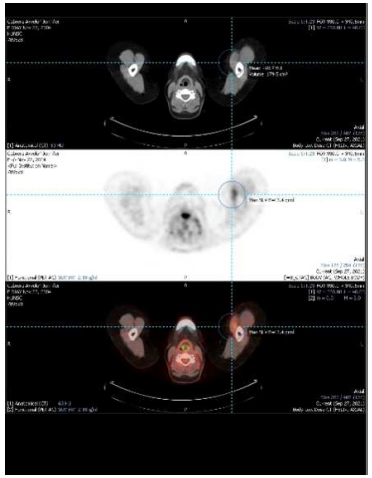

Figure 3: PET-CT is positive with increased FDG metabolism.

- Surgical biopsy/excision showing **Extraskeletal Ewing Sarcoma** of the soft tissues with involvement of the dermis and hypodermis by a proliferation of small round tumor cells. Deep margin positive. **CD99+**, **Fli1+**, CLAE1/AE3+, EMA+. **EWSR1 rearrangement** detected. Treatment: chemotherapy according to the EuroEwing 2012 therapeutic protocol. Consideration to widen surgical margins after induction. Currently under follow-up by pediatric oncology-hematology. Event-free-survival: 54 months.

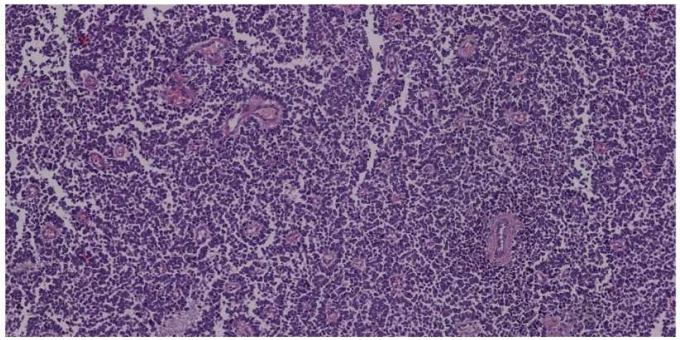

Figure 4: H&E stain (20x) showing a proliferation of small, round, blue, monomorphic cells with Homer-Wright rosette formation.

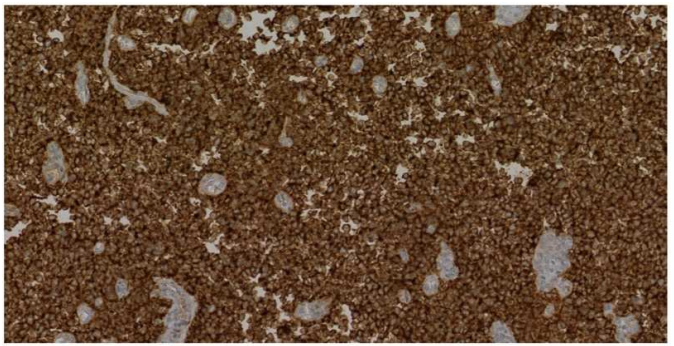

Figure 5: Typical membranous expression of CD99 observed in the tumor sample (20x).

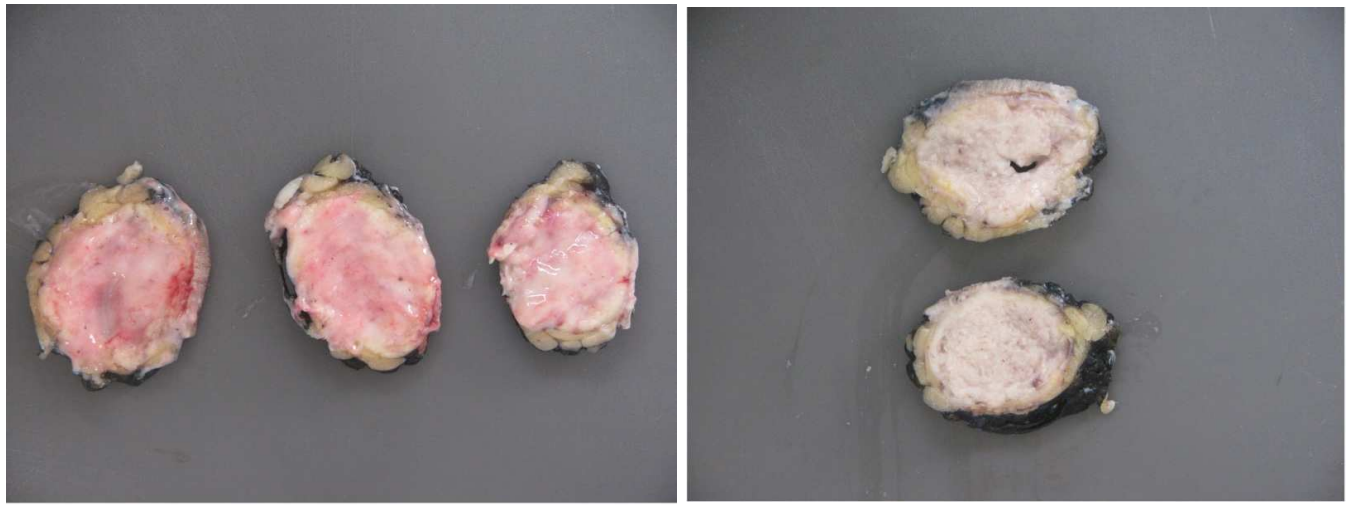

Figure 6. Fresh (A) and fixed (B) macroscopic images of the lesion, showing a well-defined, white-brown coloration with a soft consistency on cut section.

FISH
EWSR1

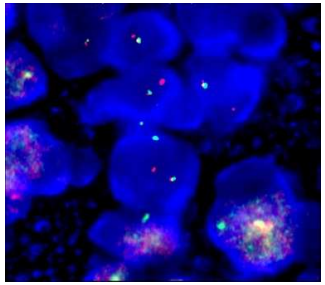

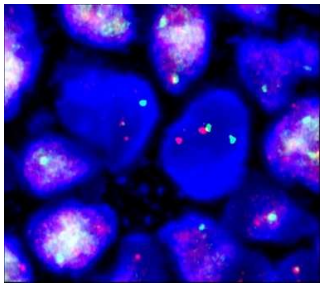

EWSR1 break-apart FISH analysis was performed, revealing rearrangement of the EWS gene (22q12).

CASO 11:

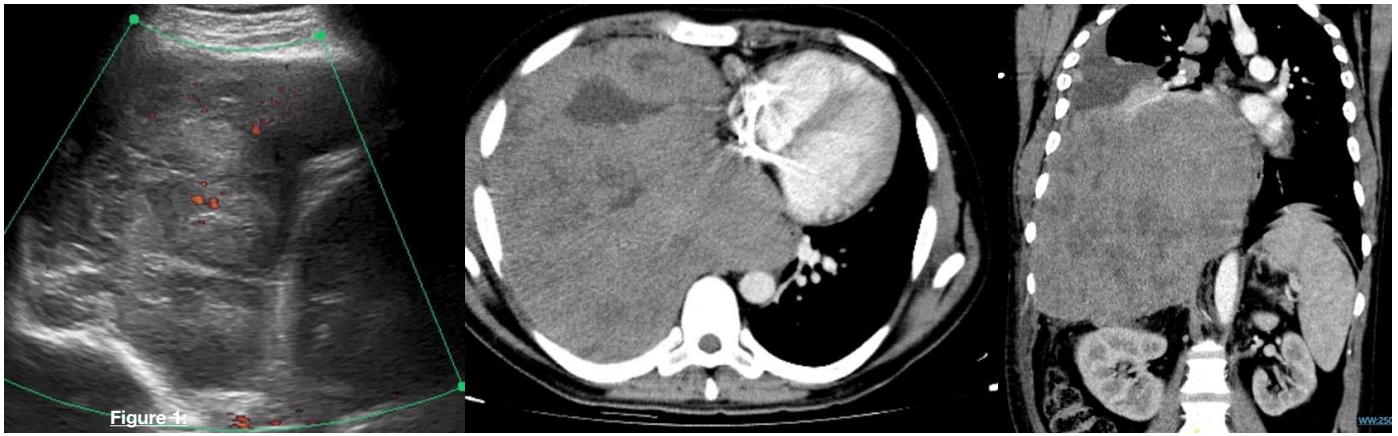

A 30-year-old man with right paravertebral pain at the L1-L2 level for 3-4 months, continuous, penetrating, waking him at night, and associated with fever. Appearance of a lump in the right renal area. PMH: right ear cervicotomy (benign lesion?), hypertension, smoker. **Figure 1:** Abdominal-pelvic ultrasound showing a large right suprarenal vs. retroperitoneal mass, heterogeneous and vascularized. Ipsilateral pleural effusion. **Figures 2:** Total body contrast-enhanced CT in axial and **Figure 3:** CT in coronal planes showing a large heterogeneous retroperitoneal mass measuring 20 x 19 x 29 cm with invasion of the right pleura and ribs, containing areas of necrotic-cystic degeneration—associated mediastinal, celiac, and retroperitoneal lymphadenopathy.

Pathological report: mesenchymal proliferation of small round cells, with morphoimmunohistochemical and cytogenetic findings consistent with **Ewing Sarcoma. EWSR1 rearrangement detected**. Treatment: GEIS 21 Ewing clinical trial systemic therapy due to disseminated disease. Initial response observed, but progression demonstrated on follow-up. Palliative chemotherapy was decided. Poor general condition, respiratory infection, deceased. Event-free-survival: 8 months.

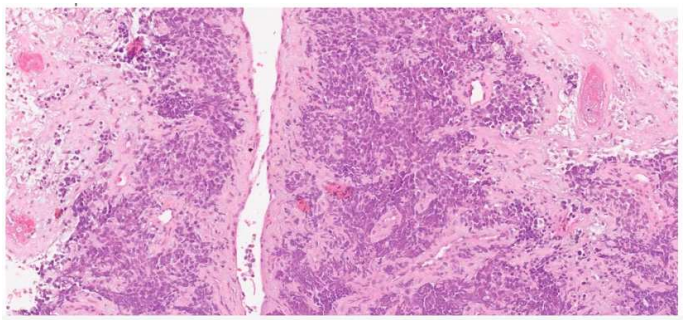

Figure 4: H&E 20x. Proliferation of small, round, blue cells arranged in nests or clusters.

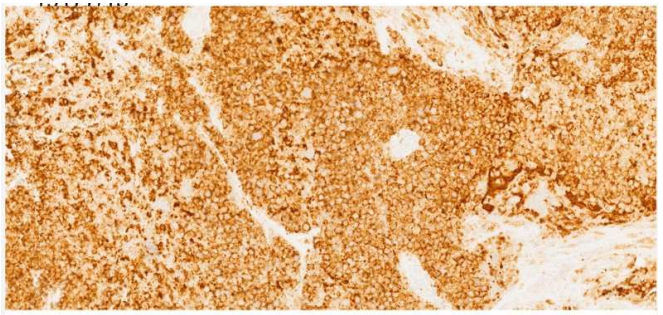

Figure 5: CD99 20x. Membranous immunostaining for CD99 in the tumor cells.

CASO 12:

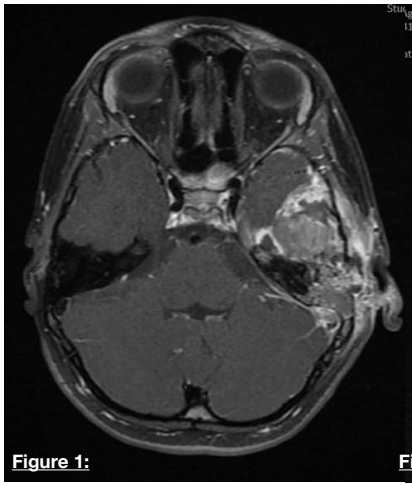

Figure 1:

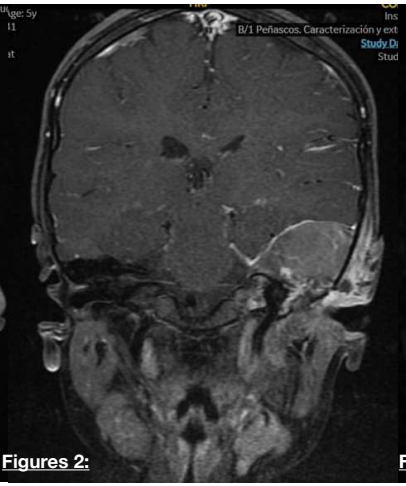

Figures 2:

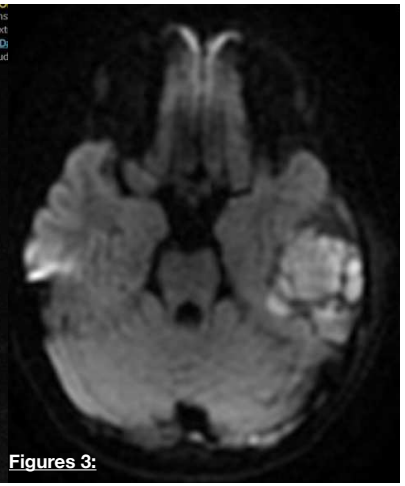

Figures 3:

5-year-old girl whose mother reports peripheral facial paralysis of the left ear lasting 1 month in the context of chronic otitis media, with multiple emergency visits without improvement despite treatment.Physical examination: Polyp in the external auditory canal (EAC) causing complete occlusion. Middle ear occlusion. CT scan showing occupation of the external ear, middle ear, and mastoid; facial nerve dehiscence in the middle ear; absence of stapes and incus. **Figure 1:** Axial MRI T1 FS and **Figure 2:** Coronal MRI T1 FS sequences with contrast showing a 4.5 x 5.5 x 4.7 cm mass centered on the left temporal bone (squama, petrous part, and mastoid) with intracranial extension displacing the temporal lobe. Thickening and mural enhancement of the left sigmoid sinus and tentorium. Edema in the left temporalis muscle, auricle, external auditory canal, and partial involvement of the parotid gland. Necrotic lymphadenopathies in the lateral cervical chains. **Figure 3:**-Axial diffusion-weighted MRI sequence demonstrating diffusion restriction.

- A surgical revision was performed, consisting of a closed mastoidectomy with tympanoplasty and facial nerve decompression. Pathology report: Immunohistochemical and molecular findings consistent with **Ewing Sarcoma** involving the external ear and the ossicular chain of the middle ear. **EWS1 rearrangement** detected. Treatment: Enrolled in the multicenter Euro-Ewing 2012 trial, assigned to arm A in the first randomization, followed by radiotherapy. The patient is currently under follow-up and in complete remission. Event-free-survival: 10 years and 3 months.

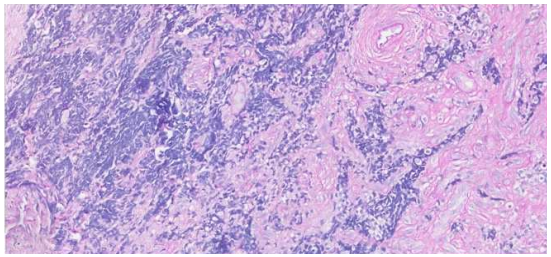

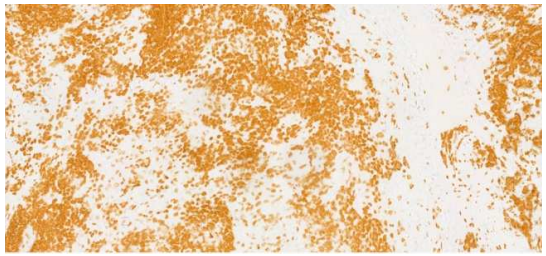

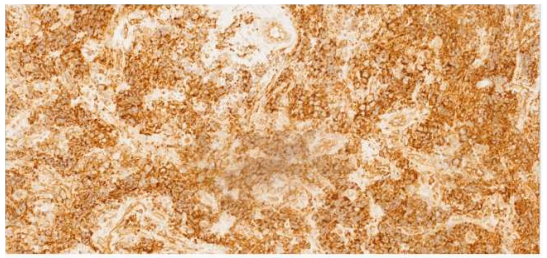

Figure 4: HE 20x. Proliferation of small, round, blue cells arranged in nests or clusters.
Figure 5: CD99 20x. Membranous immunostaining for CD99 in tumor cells.
Figure 6: FLI1 20x. Nuclear immunostaining for FLI1 in tumor cells.

RESULTS OR FINDINGS:

75% of patients were women, with a mean age of 30 years (28 years if we include the 5-year-old girl with petrous bone and ear involvement).

Symptoms depended on tumor location; 40% of patients reported the presence of a mass.

Tumor locations were distributed as follows: 16,7% in the kidney, 16,7% in the thoracopulmonary region, 25% soft tissue (1 case in dermis-hypodermis), and one case each in the intestine, retroperitoneum, petrous bone and ear, lumbosacral foramen, and adrenal gland.

Imaging showed heterogeneous enhancement with hypoenhancing regions about areas of necrosis in all cases. The mean size of tumors was 10 cm. PET-CT demonstrated increased 18-FDG uptake in the most metabolically active areas of the tumor, making it a useful tool for staging.

42% of patients had metastases primarily pulmonary (60%). Lymph node metastases were detected in 20%. All patients with widespread disease died, and all patients with localized disease survived.

Molecular study revealed an aberrant fusion between EWSR1 and transcription factors, like EWSR1-FLI1 and EWSR1-ERG, except in one case, where a FUS rearrangement is observed, consistent with the literature, since this type of rearrangement is seen in only 5% of EES.

83% of patients received chemotherapy and underwent local surgical excision. 42% were treated with radiotherapy.

CONCLUSION AND LIMITATIONS:

EES is a rare cancer that belongs to the undifferentiated small round cell sarcomas of bone and soft tissue, as per the WHO classification of 2020. Molecular study is essential for correct diagnosis and treatment. EES should be considered in young patients with large, heterogeneous soft-tissue masses. Imaging plays a crucial role in diagnosis and management. Early diagnosis is important as the prognosis is poor in cases with metastatic disease.

EES is a rare entity, making it difficult to collect a large number of case studies.

BIBLIOGRAPHIC REFERENCES:

Koscielniak E. Et al. Pediatr Blood Cancer. 2021;68:e29145.
Boyce-Fappiano D et al . Oncologist. 2021 Mar;26(3):250-260.
Qureshi SS,. Pediatr Surg Int 2013; 29:1303–1309
Kinsella TJ. J Clin Oncol 1983; 1:489–495
Galyfos G. Indian J Surg (2016) 78(1):49–53
Jiang S. Cancer Manag Res. 2018 Nov 23;10:6227-6236.
Huh J. Korean J Radiol 2015;16(4):783-790
Boyce-Fappiano D et al . Oncologist. 2021 Mar;26(3):250-260.
Applebaum MA. Pediatric blood & cancer. 2012;59(4):617-620.